

The upper line of the header, Font Size 10.5 p, Line Spacing single, Paragraph Spacing After 1.2 p

The lower line of the header, Font Size 9 p, Line Spacing single, Paragraph Spacing After 1.2 p

DOI: 10.3901/CJME.2009.03.\*\*\*, available online at www.cjmenet.com; www.cjmenet.com.cn

Font Size 8 p, paragraph followed by two blank lines

# Novel 6-DOF Wearable Exoskeleton with Pneumatic Force-Feedback for Bilateral Teleoperation

Font Size 11 p, Paragraph Spacing After 8 p

Title Font Size 14 p, Line Spacing 16 p, paragraph followed by two blank lines

ZHANG Jiafan<sup>1,3\*</sup>, FU Hailun<sup>2</sup>, DONG Yiming<sup>1</sup>, ZHANG Yu<sup>1</sup>, YANG Canjun<sup>1</sup>, and CHEN Ying<sup>1</sup>

<sup>1</sup> State Key Laboratory of Fluid Power Transmission and Control, Zhejiang University, Hangzhou 310027, China

<sup>2</sup> Zhejiang Province Institute of Metrology, Hangzhou 310027, China

<sup>3</sup> National Die & Mold CAD Engineering Research Center, Shanghai Jiao Tong University, Shanghai 200240, China

Font Size 10 p, italic, paragraph followed by one blank line

Received September 8, 2008; revised January 18, 2009; accepted February 23, 2009; published electronically March 6, 2009

**Abstract:** A particular emphasis is put on a novel wearable exoskeleton arm of freedom, which is used for the robot teleoperation with the force-feedback in the unknown environment. In order to improve the force-feedback structure mechanism, the 3-revolution-prismatic-spherical (3RPS) parallel mechanism is devised from the concept of the human upper-limb anatomy and applied for the shoulder 3-DOF joint. Meanwhile, the orthogonal experiment design method is introduced for its optimal design. Aiming at enhancing the performance of teleoperation, the force feedback is employed by the pneumatic system on ZJUESA to produce the vivid feeling in addition to the soft control interface. Due to the compressibility and nonlinearity of the pneumatic force feedback system, a novel hybrid fuzzy controller for the precise force control is proposed and realized. The feasibility of the distributed control system on ZJUESA. With the results of several experiments, the feasibility of ZJUESA system and the effect of its hybrid fuzzy controller are verified.

Font Size 8 p, paragraph followed by one blank line

Font Size 9 p, paragraph followed by one blank line

**Key words:** exoskeleton arm, teleoperation, pneumatic force-feedback, hybrid fuzzy control

heading level one Font Size 12p, Paragraph Spacing Before 1 line, paragraph followed by one blank line

Font Size 9 p, paragraph followed by two blank lines

## 1 Introduction

At first look at modern society, more and more robots and automated devices are coming into our life and serve for human. But on even further, more and more mechatronic devices replace human labor. At lower levels, essentially providing routine tasks. Human control is gradually moving to higher levels just as the term human-machine symbiosis, which is coined by SHIBATA, is used to describe the master-slave teleoperation system. In the field of teleoperation of radioactive materials in a closed environment, GOERTZ, et al<sup>[2]</sup>, was the typical example. Hereafter, exoskeleton arms with force-feedback have widely developed in the fields of robot teleoperation, haptic interface to enhance the performance of the human operator, also in the exciting applications in surgery planning, personnel training, and physical rehabilitation. DUBEY, et al<sup>[3]</sup>, developed a methodology to incorporate sensor and model based computer assistance into human controlled teleoperation systems. In their approach, the human operator was retained at all phases of the teleoperation and was assisted by adjusting system parameters.

were not used in the teleoperator, specifically, the mapping of positions and velocities between the master and slave and their impedance parameters. The ESA human arm exoskeleton was developed to enable force-feedback tele-manipulation on the exterior of the international space station with redundant robotic arms<sup>[4]</sup>. In recent work<sup>[5-6]</sup>, myoelectric signal has been used to control the teleoperator arm and many new concepts were applied in teleoperation<sup>[7-10]</sup>. Several researchers from Korea National Institute of Advanced Technology (KIST) introduced the concept of the exoskeleton and designed a 3RPS parallel mechanism<sup>[11-12]</sup>. They developed an exoskeleton-type master arm, in which the force feedback was provided with the torque sensor beams and the force feedback control<sup>[14]</sup>. Likewise, the authors proposed a control model to describe the bilateral teleoperation in the view of the control theory<sup>[15-17]</sup>.

body text Font Size 10 p, except special notes, Line Spacing exactly 1.1~1.2 line for the paragraph containing a superscript or a subscript or a complex equation

Font Size 8 p, Line Spacing single

In this research, a wearable exoskeleton arm, ZJUESA, based on man-machine system is designed and a hierarchically distributed teleoperation control system is explained. This system includes three main levels: ① supervisor giving the command through the exoskeleton with the operator interface; ② slave-robot working in hazardous zone; ③ data transmission between supervisor-master and master-slave through the Internet or Ethernet. In section 2, by using the orthogonal experiment design method, the design foundation of ZJUESA and its optimal design are presented. Then in section 3, we describe a novel hybrid fuzzy control

\* Corresponding author. E-mail: caffeezhang@hotmail.com  
This project is supported by National Natural Science Foundation of China (Grant No. 50350535), National Hi-tech Research and Development Program of China(863 Program, Grant No. ##), Beijing Municipal Natural Science Foundation of China((Grant No. ##), and Zhejiang Provincial Natural Science Foundation of China((Grant No. ##)

system for the force feedback on ZJUESA. Consequently, the force feedback control simulations and experiment results analysis are presented in section 4, followed by discussions and conclusions.

## 2 Configuration of the Exoskeleton Arm System

The master-slave control is widely employed in the robot manipula... for the keyboard is the routine... master-slave control system. ... presented in this paper is shown in Fig. 1.

A paragraph is followed by a blank line, when figures follow it.

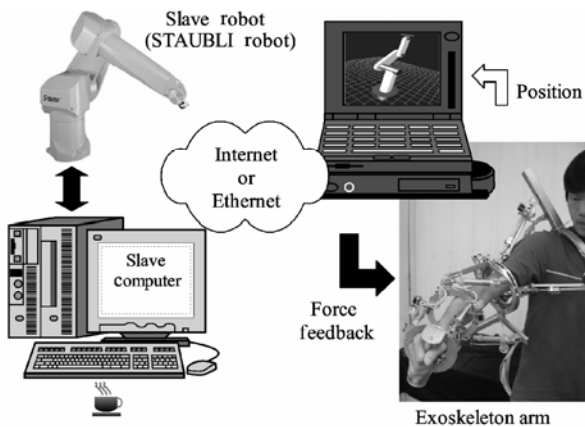


Fig. 1. Configuration of the exoskeleton arm system

In the system... the joystick as... structure mecha... and can transfer the motions of human upper arm to the slave manipulator position-control-commands through the Internet or Ethernet between the master and slave computers. With this information, the slave manipulator mimics the motion of the operator. At the same time, the force-feedback signals, detected by the 6-axis force/torque sensor on the slave robot arm end effector, are sent back to indicate the pneumatic actuators for the force-feedback on ZJUESA to realize the bilateral teleoperation.

figure title Font Size 9 p, Line Spacing exactly 11 p, Paragraph Spacing Before 0.3 p; Leave one blank line after the figure title. figure text Font Size 7.5 p

Since ZJUESA is designed by following the physiological parameters of the human upper-limb, with such a device the human operator can control the manipulator more comfortably and intuitively than the system with the joystick or the keyboard input.

## 3 Design of the Exoskeleton Arm

What we desire is an arm exoskeleton which is capable of following motions of the human upper-limb accurately and supplying the human upper-limb with proper force feedback if needed. In order to achieve an ideal controlling performance, we have to examine the structure of the human upper-limb.

### 3.1 Anatomy of human upper-limb

#### 3.1.1 Upper-limb

Recently, various... of the human upper-limb anatomy have... of the arm that sta... muscles, tendons and bones are too complex to be utilized in mechanical design of an anthropomorphic robot arm. From the view of the mechanism, we should set up a more practicable model for easy and effective realization.

heading level three Font Size 10 p, Paragraph Spacing Before 0.5 line

Fig. 2 introduces the configuration of human upper-limb and its equivalent mechanical model, which is a 7-DOF structure, including 3 degrees of freedom for shoulder (flexion/extension, abduction/adduction and rotation), 1 degree of freedom for elbow (flexion/extension) and 3 degrees of freedom for wrist (flexion/extension, abduction/adduction and rotation)<sup>[18]</sup>. The details about the motion characteristics of these skeletal joints can be obtained in Refs. [18–20]. Compared to the mechanical model, the shoulder and wrist can be considered as spherical joints and the elbow as a revolution joint. It is a good approximate model for the human arm, and the base for the design and construction of exoskeleton arm-ZJUESA.

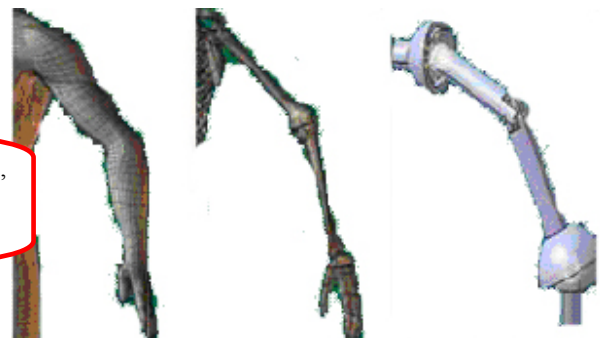


Fig. 2. Configuration of human upper limb and its equivalent mechanical model

### 3.2 Mechanism of the exo

Because the goal of this... of the human arm accurately fo... to make the best of motion scope of the human upper-limb and limit it as little as possible. A flexible structure with the same or similar configuration of human upper-limb is an ideal choice. Based on the anatomy of human upper-limb, the joint motion originates from extension or flexion of the muscle and ligament with each other to generate torque around the bones. Compared with the serial mechanism, the movements of the parallel mechanism are driven by the prismatic, which act analogically to the human muscles and ligament. Besides, using the parallel mechanism not prismatic, which act analogically to the human muscles and ligament. Besides, using the parallel mechanism not prismatic joints in the parallel mechanism lie on the surface of human upper-limb.

Leave two blank lines before a heading, when the heading follows a figure.

The 3RPS parallel mechanism is one of the simplest

mechanisms. Fig. 3 explains the principle of the 3RPS parallel mechanism. KIM, et al<sup>[11]</sup>, introduced it into the KIST design. Here we follow this concept. The two revolution degrees of freedom embodied in the 3RPS are for flexion/extension, abduction/adduction at shoulder. Its third translation degree of freedom along  $z$  axis can be used for the dimension adjustment of ZJUESA for different operators. The prismatic joints are embodied by pneumatic actuators, which are deployed to supply force reflective capability. Also displacement sensors are located along with the pneumatic actuators and the ring-shaped joints to measure their linear and angular displacements. At elbow, a crank-slide mechanism composed of a cylinder and links is utilized for flexion/extension. At wrist, since the abduction/adduction movement is so limited and can be indirectly reached by combination of the other joints, we simplify the configuration by ignoring the effect of this movement. As shown in Fig. 4, the additional ring is the same as that at shoulder for the elbow rotation. Thus our exoskeleton arm-ZJUESA has 6 degrees of freedom totally.

shoulder is the... the frame around a page number, sign. However, it is a... Width exactly 1.1 cm, Height exactly 0.4 cm, Horizontal Position 18 cm (A), saying the displ... 0.4 cm Relative to a page, Vertical Position (B), circumradius ratio... 0.4 cm Relative to a paragraph... their coupling parameters (factor  $A*B$ ,  $A*C$  and  $B*C$ ) (Table 1) and multi-targets, namely, its workspace weight size. So we use the orthogonal experiment design of a single line equation foregoing 6 key factors<sup>[21]</sup> and Eq. (1) to find the optimal target function of this problem. Line Spacing single, center; Leave one blank line after the equation.

$$Q = F\left(L_0, \theta - \theta_x, \frac{r}{R}\right) \quad (1)$$

where  $L_0$  is the initial length of the prismatics,  $R$  is the circumradius of the lower base in 3RPS mechanism,  $r$  is the circumradius of the upper base in 3RPS mechanism,  $\theta$  is the expected reachable angle at wrist,  $\theta_x$  is the reachable angle around axis. table title Font Size 9 p, bold, Paragraph Spacing After 0.3 line

**Table 1. Factors and their levels** mm

	$A$	$B$	$C$	$A*B$	$A*C$	$B*C$
1	50	0.5	150	—	—	—
2	80	0.438	160	—	—	—
3	100	0.389	170	—	—	—
4	—	—	—	—	—	—

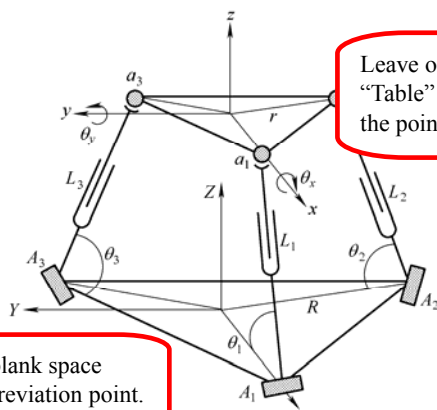


Fig. 3. 3RPS parallel mechanism

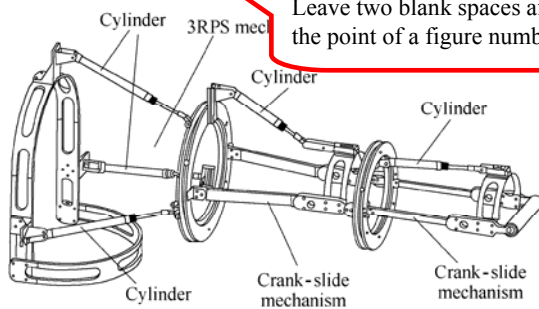


Fig. 4. Prototype of the exoskeleton arm-ZJUESA

### 3.3 Optimization design of ZJUESA

As mentioned above, the best design is to make the workspace of ZJUESA as fully cover the scope of the human upper-limb motion as possible. We employ the 3RPS parallel mechanism for the shoulder, whose workspace mainly influences the workspace of ZJUESA. The optimal design of 3RPS parallel mechanism for the

The orthogonal experiment design... the ease with which levels... efficiency. The concept of orthogonal experiment design is discussed in Ref. [21] to obtain parameters optimization, finding the setting for each of a number of input parameters that optimizes the output(s) of the design. Orthogonal experiment design allows a decrease in the number of experiments performed with only slightly less accuracy than full factor testing. The orthogonal experiment design concept can be used for any complicated system being investigated, regardless of the nature of the system. During the optimization, all variables, even continuous ones, are thought of discrete “levels”. In an orthogonal experiment design, the levels of each factor are allocated by using an orthogonal array<sup>[22]</sup>. By discretizing variables in this way, a design of experiments is advantageous in that it can reduce the number of combinations and is resistant to noise and conclusions valid over the entire region spanned by the control factors and their setting.

Table 2 describes an orthogonal experiment design array for 6 key factors<sup>[23]</sup>. In this array the first column implies the number of the experiments and factors  $A$ ,  $B$ ,  $C$ ,  $A*B$ ,  $A*B$  and  $B*C$  are arbitrarily assigned to columns respectively. From Table 2, 36 trials of experiments are needed, with the level of each factor for each trial-run indicated in the array. The elements represent the levels of each factors. The vertical columns represent the experimental factors to be studied using that array. Each of the columns contains several assignments at each level for

Leave one blank space after an abbreviation point.

Leave one blank space after the word “Table” and two blank spaces after the point of a table number.

table text Font Size 8 p, Line Spacing exactly 11 p; Leave one blank line after a table.

Leave two blank spaces after the point of a figure number.

the corresponding factors. The levels of the latter three factors are the frame around a page of the former three factors. The number, Horizontal Position namely factor  $A*B$ , are determined by the columns I, II, and III, and the elements of column V, factor  $A*C$ , has the relationship with the elements of columns I, III, and the column VI, factor  $B*C$ , lies on the columns II, III.

**Table 2. Orthogonal experiment design array L36 for 6 key factors**

Experiment number	A	B	C	A*B	A*C	B*C	Result Q
1	1	1	1	1	1	1	$Y_1$
2	1	1	2	1	2	2	$Y_2$
3	1	1	3	1	3	3	$Y_3$
4	1	1	4	1	4	4	$Y_4$
5	1	2	1	2	1	5	$Y_5$
6	1	2	2	2	2	6	$Y_6$
⋮	⋮	⋮	⋮	⋮	⋮	⋮	⋮
33	3	3	1	9	9	9	$Y_{33}$
34	3	3	2	9	10	10	$Y_{34}$
35	3	3	3	9	11	11	$Y_{35}$
36	3	3	4	9	12	12	$Y_{36}$

The relation between column IV and columns I, II is that: if level of  $A$  is  $n$  and level of  $B$  is  $m$ , the level of  $A*B$  is  $3(n-1)+m$ , where  $n=1, 2, 3$  and  $m=1, 2, 3$ .

All the cases can be expressed as follows:

- (1, 1) → 1    (1, 2) → 2    (1, 3) → 3;
- (2, 1) → 4    (2, 2) → 5    (2, 3) → 6;
- (3, 1) → 7    (3, 2) → 8    (3, 3) → 9.

The first element in the bracket represents the corresponding level of factor  $A$  in Table 1 and the latter means the corresponding level of the factor  $B$ . Factor  $A*B$  has totally 9 levels, as factor  $A$  and factor  $B$  have 3 levels, respectively.

Likewise, the relation between column V and columns I, III is

- (1, 1) → 1    (1, 2) → 2    (1, 3) → 3    (1, 4) → 4;
- (2, 1) → 5    (2, 2) → 6    (2, 3) → 7    (2, 4) → 8;
- (3, 1) → 9    (3, 2) → 10    (3, 3) → 11    (3, 4) → 12.

Also the relation between column VI and columns II, III is

- (1, 1) → 1    (1, 2) → 2    (1, 3) → 3    (1, 4) → 4;
- (2, 1) → 5    (2, 2) → 6    (2, 3) → 7    (2, 4) → 8;
- (3, 1) → 9    (3, 2) → 10    (3, 3) → 11    (3, 4) → 12.

The optimal design is carried out according to the first three columns:

$$\begin{pmatrix} I_{A_1} \\ I_{A_2} \\ \vdots \\ I_{B*C_{11}} \\ I_{B*C_{12}} \end{pmatrix} = \begin{pmatrix} 1/9 & 1/9 & 1/9 & \cdots & 0 & 0 & 0 & 0 & 0 \\ 0 & 0 & 0 & \cdots & 0 & 0 & 0 & 0 & 0 \\ \vdots & \vdots & \vdots & & \vdots & \vdots & \vdots & \vdots & \vdots \\ 0 & 0 & 0 & \cdots & 0 & 0 & 0 & 1/3 & 0 \\ 0 & 0 & 0 & \cdots & 0 & 0 & 0 & 0 & 1/3 \end{pmatrix} \begin{pmatrix} Y_1 \\ Y_2 \\ \vdots \\ Y_{35} \\ Y_{36} \end{pmatrix}, \quad (2)$$

$$K_i = \max \{I_{ij}\} - \min \{I_{ij}\}, \quad (3)$$

where  $i=A, B, C, A*B, A*C, B*C$ ;  $j$  is the number of  $i$  rank.

By Eqs. (2), (3) and the kinematics calculation of the 3RPS parallel mechanism<sup>[35]</sup>, the relationship between the target  $Q$  and the levels of factors  $L_f$  is established, as shown in Fig. 5.

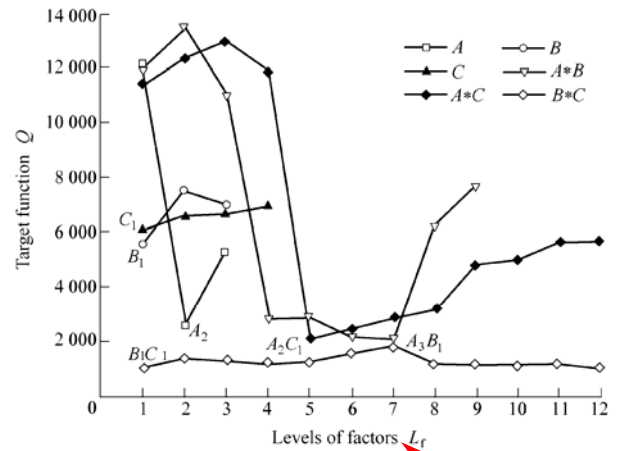


Fig. 5. Relation between levels of factors  $L_f$  and target function  $Q$ .

According to the plots in Fig. 5, the factor with bigger extreme difference  $K_i$ , as expressed in Eq. (3) has more influence on  $Q$ . In this case, it can be concluded that the sensitivity of the factors  $A*B$  and  $A*C$  are high and factors  $B*C$  and  $C$  have weak influence, since  $K_{A*B}$  and  $K_{A*C}$  are much bigger than  $K_{B*C}$  and  $K_C$ . And the set  $A_3B_1, A_2C_1, A_2, B_1, C_1, B_1C_1$  are the best combination of each factor levels. But there is a conflict with former 3 items in such a set. As their  $K_i$  have little differences between each other, the middle course is chosen. After compromising, we take the level 2 of factor  $A$ , the level 1 of factor  $B$  and the level 1 of factor  $C$ , namely  $d = 80 \text{ mm}, r/R=0.5, L_0=150 \text{ mm}$ <sup>[32]</sup>.

It is interesting to know how good the results derived from the above 36 trials are, when compared with all other possible combinations. Because of its mutual balance of orthogonal arrays, this performance ratio can be guaranteed by the theorem in non-parametric statistics<sup>[13]</sup>. It predicts that this optimization is better than 97.29% of alternatives.

Combined with the kinematics and dynamics simulation of the 3RPS parallel mechanism and ZJUESA with chosen design parameters by ADAMS, we perform the optimal design. Table 3 indicates the joint range and joint torque of





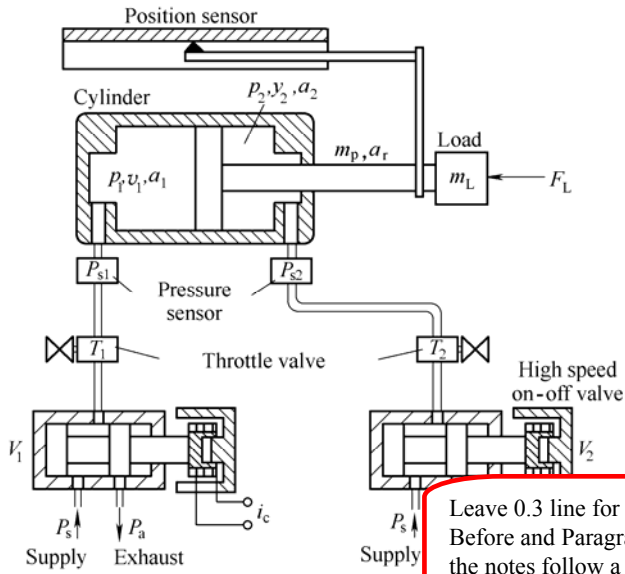


Fig. 7. Scheme of the pneumatic cylinder-valve system

$p_1, v_1, a_1$ —Pressure, volume and section area of cylinder chamber 1  
 $p_2, v_2, a_2$ —Pressure, volume and section area of cylinder chamber 2  
 $m_p$ —Mass of the piston  
 $a_r$ —Section area of rod  
 $m_L$ —Mass of load

The high-speed on-off valve components in the system, are controlled by the pulse width modulation (PWM) signals from the control units, respectively. Rather than the proportional or servo valve, this is an inexpensive and widely used method in the application of position and force control in the pneumatic system [23–28]. To simplify the control algorithm, there is just one valve on work at any moment. For instance, when a leftward force is wanted, the valve  $V_1$  works and valve  $V_2$  is out of work. Under this case, we can control the pressure  $p_1$  in chamber 1 by modifying the PWM signals. Chamber 2 connects to the atmosphere at that time and the pressure  $p_2$  inside the chamber 2 of cylinder is absolutely ambient pressure, and vice versa. At each port of the cylinder, there is a pressure sensor to detect the pressure value inside the chamber for the close-loop control. And the throttle valves are equipped for limiting the flow out of the chamber to reduce piston vibrations. In our previous work, we gave out the specific mathematic models of the system, including pneumatic cylinder, high-speed on-off valve and connecting tube [33].

However, the pneumatic system is not usually a well linear control system, because of the air compressibility and its effect on the flow line. Also the highly nonlinear flow brings troubles into the control. The conventional controllers are often developed via simple models of the plant behavior that satisfy the necessary assumptions, via the specially tuning of relatively simple linear or nonlinear controllers. As a result, for pressure or force control in such a nonlinear system, especially in which the chamber pressure vibrates rapidly, the conventional control method

can hardly have a good performance.

Fortunately, the introduction of the hybrid control method mentioned, gives out a solution to this problem. But the traditional design of the hybrid controller is always complicated and only available to the proportion or servo valve system. In our system, we figured out a kind of novel hybrid fuzzy control strategy for the high-speed on-off valves, which is much simpler and can be realized by micro control units (MCUs) in the contributed architecture. This strategy is composed of two main parts: a fuzzy controller and a bang-bang controller. The fuzzy controller provides a formal methodology for representing, manipulating, and implementing a person’s heuristic knowledge about how to control a system. It can be regarded as an artificial decision maker who performs the control decision in a closed-loop system in real time and to get the control information either from the sensor or from the decision maker who performs the control decision. The bang-bang controller is added to drive the response of the system much more quickly.

Fig. 8 shows the concept of the proposed hybrid fuzzy controller. The concept of multimode switching is applied to activate either the bang-bang controller or the fuzzy controller mode.

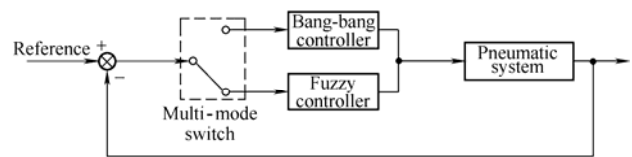


Fig. 8. Concept of the hybrid fuzzy controller

Bang-bang control is applied when the actual output is far away from reference value. In this mode, fast tracking of the output is implemented. The fuzzy controller is activated when the output is near the set point, which needs accuracy control.

In the fuzzy-control mode, we use pressure error  $e(t) = P_{ref}(t) - P_{actual}(t)$  and its change  $\dot{e}(t)$  as the input variables on which to make decisions. On the other hand, the width of the high voltage in one PWM period is denoted as the output of the controller.

As mentioned above, the PC on master site works as the supervisor for real-time displaying, kinematics calculation and exchanges the control data with the slave computer and so on. For the sake of reducing the burden of the master PC, the distributed control system is introduced. Each control unit contains a Mega8 MCU of ATMEL Inc., working as a hybrid fuzzy-controller for each cylinder respectively, and forms a pressure closed-loop control. The controller samples the pressure in chamber with 20 kHz sampling rate by the in-built analog- digital converters. These controllers keep in contact or get the differential pressure signals from the master PC through RS232, as depicted in Fig. 9. In this mode, fast tracking of the output is implemented.

Leave 0.3 line for both Paragraph Spacing Before and Paragraph Spacing After, when the notes follow a figure title.

notes Font Size 8 p, Line Spacing single; Leave one blank line after the last line of the notes.

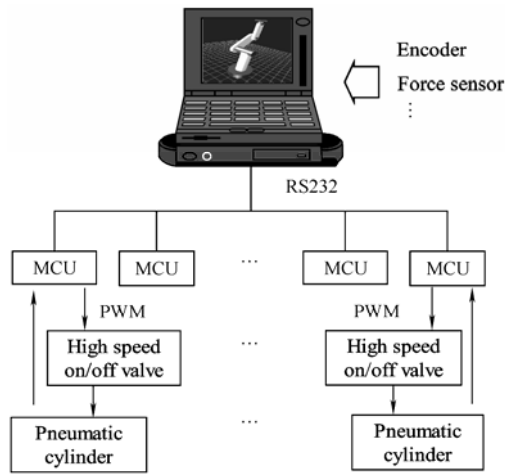


Fig. 9. Distributed control system of the master arm

### 5 Force Feedback Experiments

Fig. 10 gives out the set up of the force feedback experiments. The system includes the soft interface, data acquisition, Mega8 MCU experiment board, on-off valves, sensors of displacement and pressure, and the oscilloscope. We chose the cylinder DSNU-10-40-P produced by FESTO Inc. The soft signal generator and data acquisition are both designed in the LabVIEW, with which users may take advantage of its powerful graphical programming capability. Compared with other conventional programming environments, the most obvious difference is that LabVIEW is a graphical compiler that uses icons instead of lines of text. Additionally, LabVIEW has a large set of built-in mathematical functions and graphical data visualization and data input objects typically found in data acquisition and analysis applications.

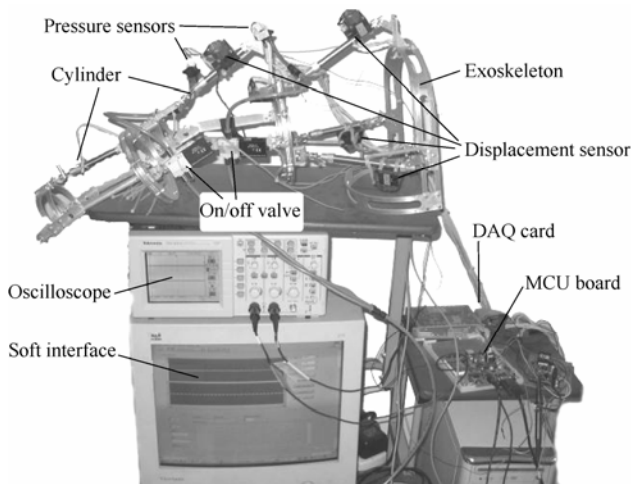


Fig. 10. Set-up of force feedback experiment

The plots in Fig. 11 give out experimental results of the chamber pressure outputs with step input signals on one joint. While at frequencies higher than 80 Hz, force is sensed through the operator's joint, muscle and tendon

receptors, and the operator is unable to respond to, and low amplitude disturbances at these frequencies. We remove reflected force signals above 80 Hz band by fast Fourier transfer (FFT) and get the smoothed curve in the plots. One is obtained by using hybrid control strategy and another is obtained by using traditional fuzzy controller without bang-bang controller. Although these two curves both track the reference well with very good amplitude match (less than 5% error) and a few milliseconds misalignment in the time profile, by comparing these two curves, it can be found that the adjust time of the curve with hybrid control strategy is less than 0.03 s, which is much less than 0.05 s of other with traditional fuzzy controller. It proves effect of the hybrid control strategy.

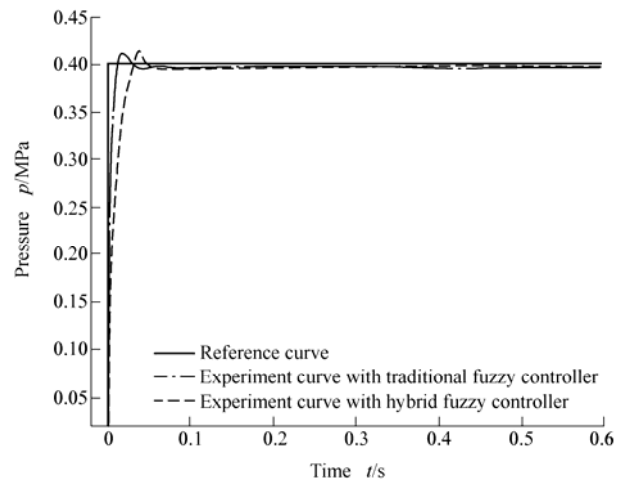


Fig. 11. Experimental results with a step signal

Fig. 12 shows the results of tracking a sinusoidal commander. This experiment is implemented to test the dynamic nature of the system. Although there is a little error and delay between the reference curve and the experiment curve, the system has good performance. According to the experiments, the system with the help of hybrid fuzzy control strategy can track an up to 5 Hz frequency sinusoidal command well.

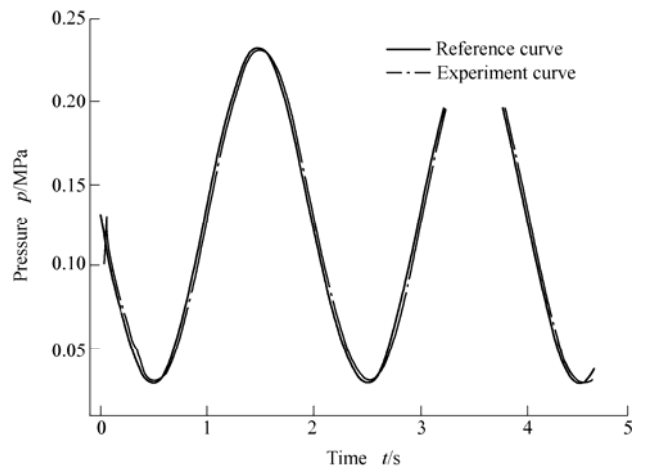


Fig. 12. Experiment results for sinusoidal pressure commands

After then, another two experiments are carried out to realize the bilateral teleoperation with simple motion, in which the slave manipulator is controlled for the shoulder abduction/ adduction (the movement of a bone away/toward the midline in the frontal plane) and extension/flexion of elbow (the movement in the sagittal plane) by the teleoperation with ZJUESA.

In the first experiment, the operator performs the shoulder abduction/adduction movement with ZJUESA, when the slave robot follows and holds up the load. With the force feedback on ZJUESA, the operator has feeling as if he holds the load directly without the mechanical structure, as shown in Fig. 13. Plots in Figs. 14, 15 show the torque and force on each joint on ZJUESA during the shoulder abduction/adduction movement from 45° to 90°(in the frontal plane) with 5 kg load. There are some remarks. In plots of Fig. 14 shoulder 3RPS-*x* means the torque around *x*-axis of 3RPS mechanism at shoulder and the same to shoulder 3RPS-*y*. Shoulder ring, elbow, wrist ring and wrist represent the torques on these joints, respectively. The characters shoulder 3RPS-1, shoulder 3RPS-2 and shoulder 3RPS-3 in Fig. 15 represent corresponding force on the cylinders on 3RPS parallel mechanism (referring to Fig. 3) with length  $L_1$ ,  $L_2$  and  $L_3$ , respectively.

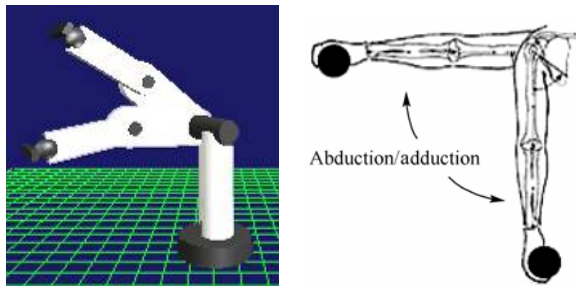


Fig. 13. Shoulder abduction/adduction teleoperation

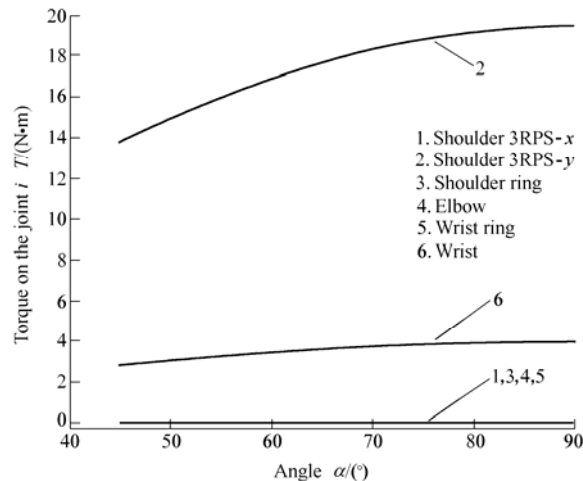


Fig. 14. Torques on the joints of the shoulder abduction/adduction for 5 kg load lifting

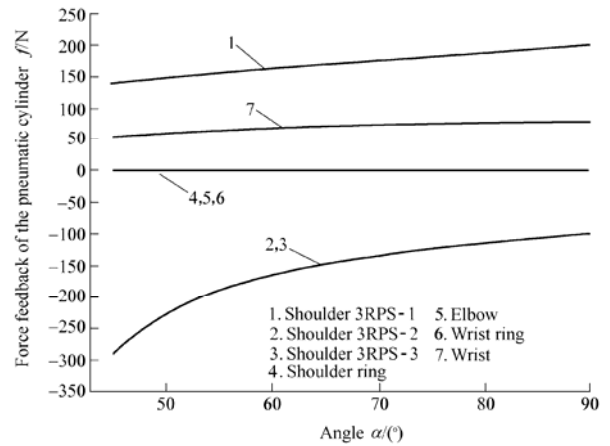


Fig. 15. Force feedback on the cylinders of the shoulder abduction/adduction for 5 kg load lifting

The operator teleoperates the slave manipulator with force feedback as if he performs for lifting a dumbbell or raising package in daily life (Fig. 16). Fig. 17 shows the moment on each joint during the process for producing the feeling of lifting a 10 kg dumbbell. Fig.18 depicts the force output of every pneumatic cylinder on ZJUESA.

All these results of experiments demonstrate the effect of ZJUESA system. ZJUESA performs well by following the motions of human upper-limb with little constrain and the pneumatic force feedback system supplies a proper force feedback tracking the reference well.

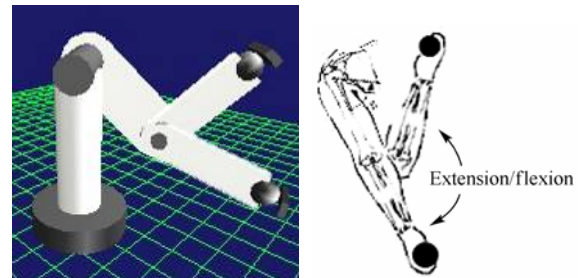


Fig. 16. Extension/flexion for elbow teleoperation

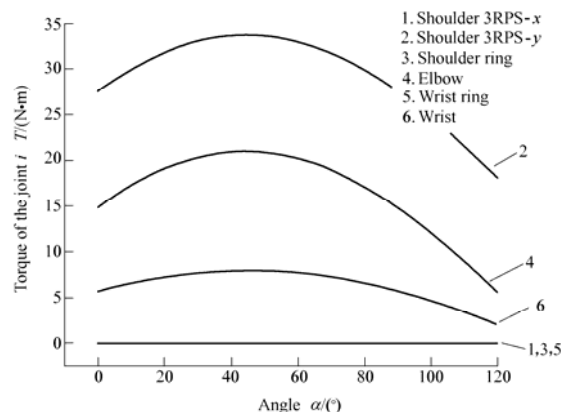


Fig. 17. Torques on the joints of the elbow extension/flexion for 10 kg load lifting



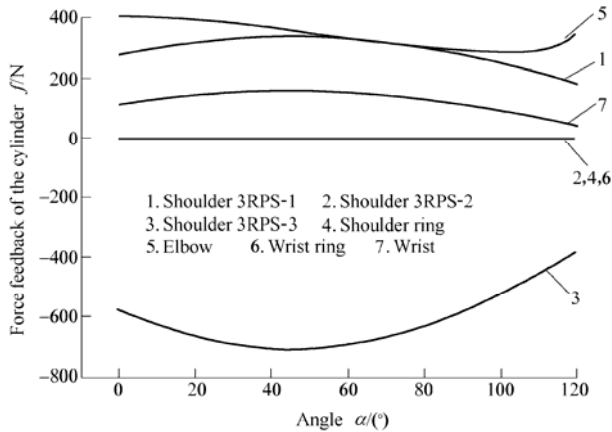


Fig. 18 Force feedback on the pneumatic cylinders of the elbow extension/flexion for 10 kg load lifting

## 6 Conclusions

(1) According to the anatomy of human upper-limb, the structure of ZJUESA is presented, which has 6 DOFs totally. 3RPS parallel mechanism analogy to the motion of muscle and ligament of human joint is employed to realize the shoulder structure with 3 degrees of freedom.

(2) The orthogonal experiment design method is employed for the optimal design. As a result a larger workspace of ZJUESA is obtained.

(3) In the interest of much more intuitive feelings in master-slave control process, the force feedback is realized simultaneously on ZJUESA by the pneumatic cylinders. And a novel hybrid fuzzy-controller is introduced in the Mega8 MCU as a unit of the distributed control system due to the non-linearity of the pneumatic system. The bang-bang control is utilized to drive the response of the system much more quickly and the fuzzy controller is activated when the output is near the set point, which needs accurate control.

(4) With sets of experiments, step, slope and sinusoidal commands are taken and the system shows a good performance, and a good agreement is found between the reference curves and experimental curves as well.

(5) The experiments of shoulder abduction/adduction and elbow extension/flexion teleoperation with force feedback are implemented. The results verify the feasibility of ZJUESA master-slave control system and the effect of the hybrid fuzzy-

Font Size 10 p

text Font Size 8 p, Line Spacing exactly 11 p

## References

- [1] SHERIDAN T B. *Automation, and human supervisory control-telerobotics*[M]. Cambridge MA: The MIT Press, 1992.
- [2] GOERTZ R C, THOMPSON R C. Electronically controlled manipulators[J]. *Nucleonics*, 1954, 12(11): 46-47.
- [3] DUBEY R, EVERETT S. Human-machine cooperative telerobotics using uncertain sensor and model data[C]//*International Conference on Robotics and Automation*, Lueven, Belgium, May 16-20, 1998: 1 615-1 622.
- [4] SCHIELE A, VISENTIN G. The ESA human arm exoskeleton for space robotics telepresence[C]//*7th International Symposium on Artificial Intelligence, Robotics and Automation in Space*, Nara, Japan, May 19-23, 2003: 21-25.
- [5] ROSEN J, HANNAFORD B, BURNS S. Neural control of an upper limb powered exoskeleton system-grant report[C]// *First NSF Robotics and Computer Vision (RCV) Workshop*, Las Vegas, USA, 2003: 26-27.
- [6] ROSEN J, BRAND M, FUCHS M B, et al. A myosignal-based powered exoskeleton system[J]. *IEEE Transaction on Systems, Man, and Cybernetics-Part A: Systems and Humans*, 2001, 31(3): 210-222.
- [7] BHARADWAJ K, HOLLANDER K W, MATHIS C A, et al. Spring over muscle (SOM) actuator for rehabilitation devices[C]//*Proceedings of the 26th Annual International Conference of the IEEE EMBS*, San Francisco, USA, September 1-5, 2004: 2 726-2 729.
- [8] KOBAYASHI H, ISHIDA Y, SUZUKI H. Realization of all motion for the upper limb by a muscle suit[C]//*Proceedings of the IEEE International Workshop on Robot and Human Interactive Communication*, Okayama, Japan, September 20-22, 2004: 631-636.
- [9] COHENA Y B, MAVROIDIS C, BOUZIT M, et al. Virtual reality robotic telesurgery simulations using MEMICA haptic system[C]// *Proceedings of SPIE's 8th Annual International Symposium on Smart Structures and Materials*, Newport, USA, March 5-8, 2001: 1-8.
- [10] NAKAI A, OHASHI T, HASHIMOTO H. 7 DOF arm type haptic interface for teleoperation and virtual reality system[C]// *Proceedings of the IEEE/RSJ International Conference on Intelligent Robots and Systems*, Victoria, Canada, October, 1998: 1 266-1 231.
- [11] KIM I, CHANG S, KIM J, et al. KIST hybrid master arm[C]// *Proceedings of the ASME Dynamic Systems and Control Division*, Nashville, USA, November 14-19, 1999: 195-204.
- [12] JEONG Y, LEE D, KIM K, et al. A wearable robotics arm with high force-reflection capability[C]//*Proceedings of the IEEE International Workshop on Robot and Human Interactive Communication*, Osaka, Japan, September 27-29, 2000: 27-29.
- [13] The triplex design group of Chinese Association of Statistics. *Orthogonal method and triplex design*[M]. Beijing: Science Press, 1987. (in Chinese)
- [14] KIM Y S, LEE J, LEE S, et al. A force reflected exoskeleton-type masterarm for human-robot interaction[J]. *IEEE Transactions on Systems, Man, and Cybernetics-Part A: Systems and Humans*, 2005, 35(2): 198-212.
- [15] LAWRENCE D A. Designing teleoperator architectures for transparency[C]// *IEEE Int. Conf. on Robotics and Automation*, Nice, France, May, 1992: 1 406-1 411.
- [16] RAJU G J. Design issues in 2-port network models of bilateral remote manipulation[C]// *Proceedings of the IEEE International Conference on Robotics and Automation*, Piscataway, NJ, USA, May 14-19, 1989: 1 313-1 321.
- [17] YOKOKOHI Y, YOSHIKAWA T. Bilateral control of master-slave manipulators for ideal kinesthetic coupling-formulation and experiment[J]. *IEEE Transactions on Robotics and Automation*, 1994, 10(5): 605-620.
- [18] TORTORA G J, GRABOWSKI S R. *Introduction to the human body-the essentials of anatomy and physiology*[M]. 5th edition. New York: John Wiley & Sons, Inc., 2001.
- [19] LENARCIC J, STANISIC M. A humanoid shoulder complex and the humeral p[C]// *Proceedings of the IEEE International Conference on Robotics and Automation*, Nice, France, May, 1992: 1 406-1 411.
- [20] VEEGER H. The effect of the glenohumeral joint[C]// *Journal of Biomechanics*, 2000, 12: 1 711-1 715.
- [21] FANG K T, MA C X. *Orthogonal and uniform experimental design*

Give his full name for a Chinese author. Avoid using an abbreviation.

- [M]. Beijing: Science Press, 2000. (in Chinese)
- [22] AMAGO T. Sizing optimization using response surface method in FOA[J]. R&D Review of Toyota CRDL, 2002, 37(1): 1-7.
- [23] Shanghai Science and Technology Station. *The method of the orthogonal experiment design-multi factors experiment method*[M]. Shanghai: Shanghai People's Press, 1975. (in Chinese)
- [24] YANG C J, NIU B, ZHANG J F, et al. Different structure based control system of the puma manipulator with an arm exoskeleton[C]// *Proceedings of the IEEE Conference on Robotics, Automation and Mechatronics*, Singapore, December 12-15, 2004: 572-577.
- [25] KAITWANIDVILAI S, PARNICHKUN M. Force control in a pneumatic system using hybrid adaptive neuro-fuzzy model reference control[J]. *Mechatronics*, 2005, 15(1): 23-41.
- [26] AHN K, YOKOTA S. Intelligent switching control of pneumatic actuator using on/off solenoid valves[J]. *Mechatronics*, 2005, 15(6): 683-702.
- [27] SHIH M C, MA M A. Position control of a pneumatic cylinder using fuzzy PWM control method[J]. *Mechatronics*, 1998, 8(3): 241-253.
- [28] MESSINA A, GIANNOCARO N I, GENTILE A. Experimenting and modelling the dynamics of pneumatic actuators controlled by the pulse width modulation (PWM) technique[J]. *Mechatronics*, 2005, 15(7): 859-881.
- [29] XU W L, WU R H. Lyapunov's indirect method for stability analysis of fuzzy control system[J]. *Journal of Hunan University (Natural Sciences)*, 1998, 31(3): 86-89. (in Chinese)
- [30] JENKINS D, PASSINO K M. An introduction to nonlinear analysis of fuzzy control systems[J]. *Journal of Intelligent and Fuzzy Systems*, 1999, 7(1): 75-103.
- [31] BARTH E J, ZHANG J L, GOLDFARB M. Control design for relative stability in a PWM-controlled pneumatic system[J]. *Journal of Dynamic Systems, Measurement, and Control*, 2003, 125(9): 504-508.
- [32] ZHANG J F, YANG C J, CHEN Y. Use orthogonal experimental method to the optimal design for exoskeleton arm[J]. *WEASA Transactions on Systems*, 2007, 6(6): 1 095-1 101.
- [33] CHEN Y, ZHANG J F, YANG C J, et al. Design and hybrid control of the pneumatic force-feedback systems for arm-exoskeleton by using on/off valve[J]. *Mechatronics*, 2007, 17(7): 325-335.
- [34] CHEN Y, ZHANG J F, YANG C J, et al. The workspace mapping with deficient DOF space for the puma 560 robot and its exoskeleton-arm by using orthogonal experiment design method[J]. *Robotics and Computer Integrated Manufacturing*, 2006, 23(4): 478-487.
- [35] HUANG Z. *The mechanism and control theory of the parallel robot*[M]. Beijing: China Machine Press, 1997. (in Chinese)

### Biographical notes

ZHANG Jiafan, born in 1980, is currently a master candidate in State Key Laboratory of Fluid Power Transmission and Control, Zhejiang University, China. He received his bachelor degree from Shanghai Jiaotong University, China, in 2003. His research interests include man-machine system and intelligent robotics. Tel: +86-571-87953096; E-mail: caffeezhang@hotmail.com

FU Hailun, born in 1977, is currently an engineer in Zhejiang Province Institute of Metrology, China. He received his master degree on mechatronics in Zhejiang University, China, in 2006.

DONG Yiming, born in 1983, is currently a master candidate in State Key Laboratory of Fluid Power Transmission and Control, Zhejiang University, China. E-mail: tim830528@163.com

ZHANG Yu, born in 1985, is currently a master candidate in State Key Laboratory of Fluid Power Transmission and Control, Zhejiang University, China. E-mail: zhangyu\_mm@hotmail.com

YANG Canjun, born in 1969, is currently an professor in Zhejiang University, China. He received his PhD degree from Zhejiang University, China, in 1997. His research interests include mechatronics engineering, man-machine system, robotics and ocean engineering. Tel: +86-571-87953759; E-mail: ycj@sfp.zju.edu.cn

HEN Ying, born in 1962, is currently a professor and PhD candidate supervisor in State Key Laboratory of Fluid Power Transmission and Control, Zhejiang University, China. His main research interests include mechatronics engineering, fluid power transmission and control, ocean engineering. E-mail: ychen@zju.edu.cn

### Appendix

Appendix and supplement both mean material added at the end of a book. An appendix gives useful additional information, but even without it the rest of the book is complete: In the appendix are forty detailed charts. A supplement, bound in the book or published separately, is given for comparison, as an enhancement, to provide corrections, to present later information, and the like: A yearly supplement is issue.

text Font Size 9 p, Line Spacing exactly 11 p; Leave one blank line after a paragraph.

Font Size 12 p

text Font Size 10 p